



# The Theoretical Investigation of InGaAs/GaAs Quantum Well Lasers Systems

Sinan Yasar (Corresponding author)  
Department of Physics, Mustafa Kemal University  
Hatay 31030, Turkey  
Tel: +90 326 2455845 E-mail: [sinan\\_yasar@msn.com](mailto:sinan_yasar@msn.com)

Ismail Bilican  
Science and Technology Application and Research Center, Aksaray University  
Aksaray 68100, Turkey  
Tel: +90 382 2882758 E-mail: [bilicanismail@gmail.com](mailto:bilicanismail@gmail.com)

Murat Oduncuoglu  
Technical Sciences Vocational School of Higher Education, University of Gaziantep  
Gaziantep 27310, Turkey  
Tel: +90 342 3173637 E-mail: [muratodn@hotmail.com](mailto:muratodn@hotmail.com)

Sedat Agan  
Department of Physics, Kirikkale University  
Kirikkale 71450, Turkey  
Tel: +90 318 3574088 E-mail: [sedatagan@hotmail.com](mailto:sedatagan@hotmail.com)

Ihsan Uluer  
Department of Electrical and Electronics Engineering, Karabuk University  
Karabuk 78050, Turkey  
Tel: +90 370 4331563, E-mail: [ihsanuluer@gmail.com](mailto:ihsanuluer@gmail.com)

## Abstract

The host material system for long wavelength novel dilute nitride devices is InGaAs/GaAs quantum well systems. This system is the starting point to study the effect of nitrogen incorporation for 1.3-1.5  $\mu\text{m}$  wavelength emission devices. The material gain and light-current-voltage (L-I-V) characteristics of InGaAs/GaAs Fabry-Parot type quantum well laser structures were theoretically investigated. The effect of temperatures and carrier concentrations on optical gain and L-I-V characteristics of nitrogen-free systems are simulated.

**Keywords:** Fabry-Parot structure, Opto-electronics devices, Optical gain, Quantum well lasers, Semiconductor laser

## 1. Introduction

Recently, use of semiconductor lasers has dramatically increased. The optical characteristics, small size, and performance of these devices have allowed many new uses to be commercialized. Semiconductor quantum well lasers have become one of the most popular types of laser devices. Their widespread applicability,



portability and potential commercial perspectives have drawn a focused attention of many research groups and companies worldwide. High-performance GaAs based strained QW lasers will still be the subject of intense research and development for the realization of low cost optical communication systems. The InGaAs (Dieter & Nikolai 2003; Dybiec *et al.* 2004; Torchynska 2009; Hulicius *et al.* 2008) InAlAs (Liu *et al.* 2003; Chen *et al.* 2009), AlGaAs (Zhang *et al.* 2002) and dilute nitrides GaInNAs (Shan *et al.* 1999) materials were used with the aim to shift the emission peak towards the telecommunication wavelength of 1.30  $\mu\text{m}$ . InGaAs has attracted interest also as the active channel, attributed to its inherent electrical properties including narrower bandgap and high electron mobility and velocity (Smith *et al.* 2003).

The main factors driving the surge in the role played by semiconductor lasers are the invention of novel semiconductor devices. The better theoretical understandings of these novel devices, the electronic and optical characteristics of these laser devices are studied. The characteristic of light-current-voltage (LIV) is fundamental parameters to determine the operating properties of these laser systems. In this study, the carrier concentrations dependence of gain and light-current-voltage (LIV) characteristics of InGaAs/GaAs quantum well laser systems at different temperatures are investigated.

## 2. The Model

In our calculations, the band structure and parameters are calculated by using 8x8 band KP methods. In these calculations, LaserMOD™ (Rsoft Design 2005) that is self-consistent laser diode simulation program is used. This program solves optical, electronic, and thermal properties of semiconductor lasers and similar active devices. In the band structure calculations, 8x8 band Kronig-Penney (KP) model with axial approximation is used for determining the semiconductor quantum well laser systems. In KP method, one conduction- and three valence-bands are considered with including the spin degeneracy. In our calculations, the temperature dependence of the band gap is calculated by using Varshni Equation (1967) as

$$E_g(T) = E_g(T_{ref}) + \frac{\alpha T^2}{T + \beta} - \frac{\alpha T_{ref}^2}{T_{ref} + \beta} \quad (1)$$

where  $E_g$  is the bandgap energy,  $T$  is temperature,  $T_{ref}$  is the reference temperature (0 or 300K),  $\alpha$  and  $\beta$  are constants. The relevant parameters  $P$  for the  $\text{In}_x\text{Ga}_{1-x}\text{As}$  and  $\text{Al}_x\text{Ga}_{1-x}\text{As}$  ternary material systems are linearly interpolated between the parameters of the relevant binary semiconductors. The parameters used in the calculations are given in Ref. (Vurgaftman *et al.* 2001). The bandgap, conduction band-, and valence band-offsets of quantum well is play an important role for determining the electric and optical properties of these systems. In the implementation of the KP calculation, the Hermitian form of the effective mass equation is solved after Fourier expansion in the  $y$ -direction. The growth direction is supposed to be along the  $y$ -axis. The growth direction of the heterostructure omitting interactions of carriers with other quasi particles in the semiconductor material. In addition, the masses for electrons and holes are determined from the band structure as obtained from the KP calculations. Many-body interactions of the optically created electrons and holes lead to the band-gap renormalization which in turn determines the absorption spectra of such systems. The carrier density dependent band gap renormalizations are derived from a local density approximation for the Coulomb self-energies. These calculated renormalizations are contained in the band edges. Subband energies  $E_j$ , for subband  $j$ , and the respective wave functions are obtained by solving Schrodinger's equation. The total carrier concentration is given by the sum of carriers in bound states and propagating continuum states,  $n_{e/h} = n_{e/h}^{2D} + n_{e/h}^{3D}$  in quantum wells. The bound carriers are the sum over individual subband contributions. The carrier densities are related to the Fermi levels by in bulk regions:

$$n_{e/h}^{3D} = 2 \left( \frac{m_{e/h} k_B T}{2\pi\hbar} \right)^{3/2} F_{1/2} \left( \frac{\pm F_{e/h}}{k_B T} \right) = N_{C/V} F_{1/2} \left( \frac{\mp}{k_B T} \right) \quad (2)$$

where  $F_{1/2}$  is the Fermi integral of order one-half,  $F_{e/h}$  are the Fermi energies of electrons and holes,  $E_{C/V}$  are the conduction and valence band edges.

The material gain is the most important requirement for the realization of a semiconductor laser because it describes the optical amplification in the semiconductor material. The optical gain is due to stimulated emission associated with light emission created by recombination of electrons and holes. This is a complex many-body problem of interacting photons, electrons, and holes. Omitting interactions of carriers with other quasi particles, the spontaneous emission  $u$  and gain  $g$  can be written as

$$u(\omega) = \sum_{i,j} \int dE \langle \psi_{e,i} | \psi_{h,j} \rangle (B g_{red})_{i,j} f_{e,i}^{2D}(E) f_{h,j}^{2D}(E) L_{i,j}(\hbar \omega - E) \quad (3)$$

$$g(\omega) = \sum_{i,j} \int dE \langle \psi_{e,i} | \psi_{h,j} \rangle (B_{21} g_{red})_{i,j} (f_{e,i}^{2D}(E) + f_{h,j}^{2D}(E) - 1) L_{i,j}(\hbar \omega - E) \quad (4)$$

where  $f_{e,c}(E)$  are the quasi-Fermi levels for electrons and holes, which can be determined by normalizing the total number of electrons or holes,  $L_{i,j}$  is the Lorentzian broadening that is used to model the collision broadening:

$$L_{i,j}(E) = \frac{\Delta E / 2}{(\hbar \omega - E)^2 + (\Delta E / 2)^2} \Theta(E - E_g) \quad (5)$$

The gain calculation is done by using these formulas. Accordingly, understanding the processes and the results are major objectives as being a basic requirement for device optimization.

### 3. Result and Discussion

The laser device used in this paper is designed as Fabry – Parot type. The InGaAs/GaAs laser structure has a cavity length of 500  $\mu\text{m}$  and the reference temperature is 300 K. The reflectivities of the two end facets are 37%. The 104-nm thick  $\text{Al}_{0.1}\text{Ga}_{0.9}\text{As}$  substrate is used as cladding. The active region consists of 16-nm  $\text{In}_{0.18}\text{Ga}_{0.82}\text{As}$  quantum wells with 1.27% strain.

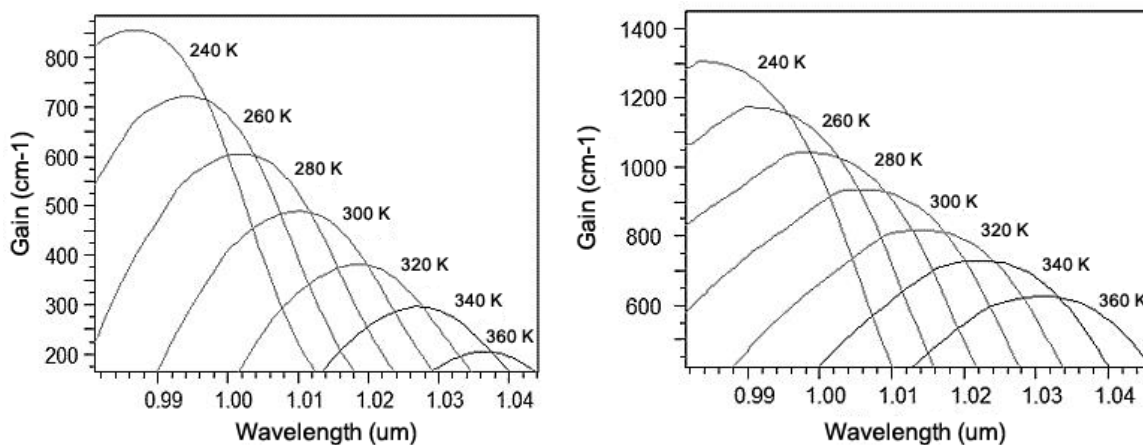


Figure 1. The material gain spectra of  $\text{In}_{0.18}\text{Ga}_{0.82}\text{As}/\text{GaAs}/\text{AlGaAs}$  material system with sheet carrier concentrations of (left one)  $N=2.5 \times 10^{12} \text{ cm}^{-2}$  and (right one)  $N=3.5 \times 10^{12} \text{ cm}^{-2}$  as a function of temperature.

The material gain versus wavelength with two different carrier concentrations over the temperature range from  $-30^{\circ}\text{C}$  to  $90^{\circ}\text{C}$  are obtained from the simulation and plotted in Figure 1. For InGaAs/GaAs/AlGaAs structure with  $2.5 - 3.5 \times 10^{12} \text{ cm}^{-2}$  carrier concentrations, the effects of temperature on material gains are investigated. As the temperature increases the peak of the gain decreases and blue shifted. In comparison, the material gain increases with increasing carrier concentration in the order of 1.6. The results of peak gain versus temperature are shown in Figure 2.

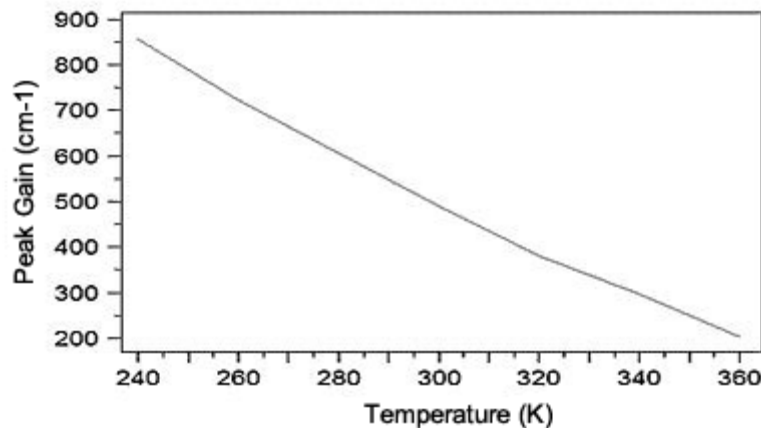


Figure 2. The temperature dependence of peak gain spectra with sheet carrier concentrations of  $N=2.5 \times 10^{12} \text{ cm}^{-2}$

The peak gain is determined from the maximum of the gain spectrum and plotted as a function of the temperature. As expected, when the temperature increases. The decrease in radiative recombination with temperature is effective in these systems. As a decrease of gain with increasing temperature has to be compensated by an increase of carrier density within the active layers, the threshold injection current increases with temperature.

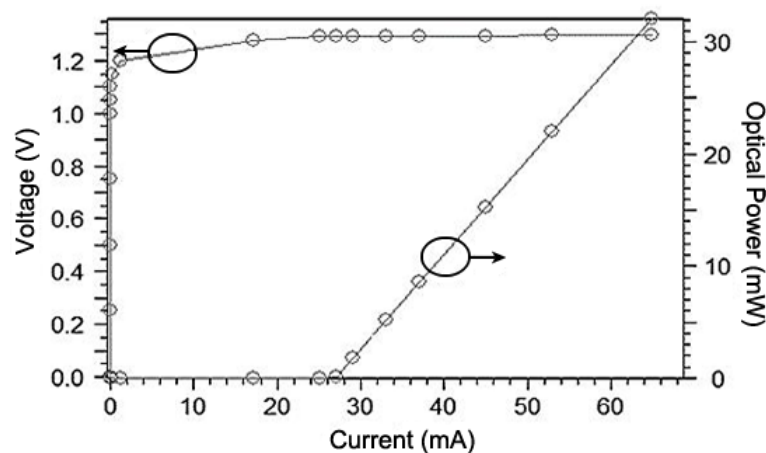


Figure 3. Light-current-voltage (L-I-V) characteristics of the device at 300 K.

Light output and voltage versus current (L-I-V) performance of designed semiconductor laser system at 300 K is shown in Figure 3. As the injection current is increased above its threshold value, lasing results. The



semiconductor laser is unique in that the population inversion required reaching lasing threshold results from electrical charge injection into the active region. From Figure 3., the threshold current is about 27 mA for the laser and gets active and lasing is evidenced by a sharp increase in output power is about 32 mW at 65 mA starting value.

#### 4. Conclusion

In summary, the temperature and carrier concentration dependence of gain and light-current-voltage (L-I-V) spectra of InGaAs/GaAs quantum well laser are presented. It is shown that the material gain decreases with increasing temperature. The effects of the carrier concentration of designed quantum well laser structure are discussed. The gain and LIV curve of the host materials for long wavelength dilute nitride systems are investigated.

#### Acknowledgment

We thank to Light Tec. and Synopsys / RSoft Company for their permission for using the LaserMOD™ devices.

#### References

- Chen, J.F. et al. (2009), "Influence of thermal annealing on the electron emission of InAs quantum dots containing a misfit defect state", *Journal of Applied Physics* **105**, 63705.
- Dieter, B. & Nikolai, L. (2003), "Quantum dots: lasers and amplifiers", *Journal of Physics: Condensed Matter* **15**, R1063.
- Dybiec, M. et al. (2004), "Scanning photoluminescence spectroscopy in InAs/InGaAs quantum-dot structures", *Applied Physics Letters* **84**, 5165-5167.
- Hulcius, E. et al. (2008), "Growth and properties of InAs/In<sub>x</sub>Ga<sub>1-x</sub>As/GaAs quantum dot structures", *Journal of Crystal Growth* **310**, 2229-2233.
- LaserMOD by Rsoft Design (2005), "Photonic device design software tool".
- Liu, H.Y. et al. (2003), "Engineering carrier confinement potentials in 1.3- $\mu$ m InAs/GaAs quantum dots with InAlAs layers: Enhancement of the high-temperature photoluminescence intensity", *Applied Physics Letters* **83**, 3716-3718.
- Shan, W. et al. (1999), "Band anticrossing in GaInNAs alloys", *Phys. Rev. Lett.* **82**, 1221-1224.
- Smith, P. et al. (2003), "Progress in GaAs metamorphic HEMT technology for microwave applications", in *Gallium Arsenide Integrated Circuit (GaAs IC) Symposium, 25<sup>th</sup> Annual Technical Digest 2003 IEEE*.
- Torchynska, T.V. (2009), "Exciton capture and thermal escape in InAs dot-in-a-well laser structures", *Superlattices and Microstructures* **45**, 349-355.
- Varshni, Y.P. (1967), "Temperature dependence of the energy gap in semiconductors", *Physica*, **34**, 149-154.
- Vurgaftman, I., Meyer, J. & Ram-Mohan, L. (2001), "Band parameters for III-V compound semiconductors and their alloys". *Journal of applied physics* **89**, 5815-5875.
- Zhang, Z.Y. et al. (2002), "Photoluminescence study of self-assembled InAs/GaAs quantum dots covered by an InAlAs and InGaAs combination layer", *Journal of Applied Physics* **92**, 511-514.